Journal of
Materials Chemistry B

Accepted Manuscript

This is an *Accepted Manuscript*, which has been through the Royal Society of Chemistry peer review process and has been accepted for publication.

Accepted Manuscripts are published online shortly after acceptance, before technical editing, formatting and proof reading. Using this free service, authors can make their results available to the community, in citable form, before we publish the edited article. We will replace this *Accepted Manuscript* with the edited and formatted *Advance Article* as soon as it is available.

You can find more information about *Accepted Manuscripts* in the Information for Authors.

Please note that technical editing may introduce minor changes to the text and/or graphics, which may alter content. The journal's standard Terms & Conditions and the Ethical guidelines still apply. In no event shall the Royal Society of Chemistry be held responsible for any errors or omissions in this *Accepted Manuscript* or any consequences arising from the use of any information it contains.

ROYAL SOCIETY OF CHEMISTRY

www.rsc.org/materialsB

Journal of

Materials Chemistry B

RSC Publishing

ARTICLE

Thermally Activated Reversible Shape Switch of Polymer Particles

Cite this: DOI: 10.1039/x0xx00000x

Tao Gong[+], Kun Zhao[+], Wenxi Wang, Hongmei Chen, Lin Wang, Shaobing Zhou*

Received 00th January 2012,
Accepted 00th January 2012

DOI: 10.1039/x0xx00000x

www.rsc.org/

The particles that can reversibly switch shape in response to an environment stimulus are preferable in controlling the performance of drug carriers. In this work, we present a facile strategy towards the design and fabrication of polymer particles which can switch their shape reversibly on the basis of a biocompatible and biodegradable polymer network containing well-defined six-arm poly(ethylene glycol)-poly(ε-caprolactone) (6A PEG-PCL). These polymer particles have a capacity of reversible changing shape from spherical to elliptical either extracellularly or intracellularly with the cyclic heating and cooling between 43 ℃ and 0 ℃ under a stress-free condition via the reversible two-way shape memory effect (2W-SME) of polymer matrix. This study of the shape-switching particles opens up exciting possibilities in engineering dynamically shape-switching drug delivery carriers to either avoid or promote phagocytosis.

Introduction

Polymeric particles have been widely used as carriers for drug delivery and medical imaging since they have an ability of delivering their cargos preferentially into targeted location, and in turn enhance the therapeutic and diagnostic efficacy. [1-3] Particle shape has been recently recognized as an important design parameter [4] because they have a strong impact on carrier performances, such as phagocytic internalization, [5-8] transport in the vasculature,[9] blood circulation half-life,[10, 11] and targeting efficiency.[12, 13] The optimization of particle geometry is very vital to enhance particle functions in biomedical application. The general approaches for synthesizing particles have involved "bottom-up" chemical processes[14-16] and "top-down" fabrication techniques.[17, 18] To date, the one-way shape memory effect of microparticles has received more and more attention. Andreas Lendlein et al report a strategy to prepare and evaluate microsized SMP model particles, processes for the preparation of SMP MP-loaded water-soluble polymer films with tailored mechanical properties were developed and applied for programming the SMP MP to a temporary ellipsoid shape by film stretching.[19, 20] Biqiong Chen et al report a polymer composites with excellent water-active shape-memory effects (SMEs) were successfully prepared using polyvinyl alcohol (PVA) submicron particlesas the SME-activating phase and thermoplastic polyurethane (TPU) as the resilient source and matrix.[21] Herein, we will present a facile strategy towards the design and fabrication of polymer particles which can switch their shape reversibly upon exposure to a thermo stimulus. The shape-switching function is endowed by the reversible two-way shape memory effect (2W-SME) of polymer matrix. These changeable shapes of the polymer particles are programmed from spherical shape to predesigned shapes using a modified film-stretching technique similarly described by Champion et al.[5] Unlike other approaches mentioned above, our strategy to achieve various shapes of particles is a combination of simple processing technique with smart-responsive material.

Shape memory polymers (SMPs) are an exciting class of smart materials and represent greatly potential applications in intelligent biomedical devices for their ability to change their shape on demand in response to a tailored environmental stimulus.[22-25] Among these stimuli-responsive SMPs, thermally induced SMPs are frequently investigated, and their shape change usually displays a one-way character. They can only change their shape in a predefined pattern

Journal of Materials Chemistry B Accepted Manuscript

from a single temporary shape (B) to another permanent shape (A) through heating these materials above a characteristic temperature, commonly defined as transition temperature (T_{trans}).[26-28] The shift of the dual shape is irreversible, and any one-way shape memory cycles going from the original shape to the previous temporary shape always requires the application of an external mechanical manipulation.[29] As a result, their applicability can be restricted due to the fact that for some applications such as the realization of actuators, artificial muscles and controlled drug release on demand, a reversible shape change can be highly required upon cooling and heating.[30, 31]

Most recently smart materials with two-way shape memory effect (2W SME) have attracted considerable attraction because they are capable of undergoing reversible dimensional variations between two distinguished geometries when they are exposed to an external stimulus. Semicrystalline polymer networks have nowadays been reported as an interesting solution towards 2W SME since their synthesis is easy and cheap in contrast to liquid crystalline elastomers or other solutions.[32-37] However, most of reported 2W SME were realized under application of a constant stress when these materials were subjected to cooling-heating cycles. If they are utilized in the body, the constant stress cannot be carried out conveniently. Moreover, the biocompatibility need to be seriously considered if the material is designed for biomedical applications. Furthermore, along with the trend towards miniaturization, small-scale actuators for SME use will be required.[38, 39] Micrometer-sized carriers of switchable shape may allow a tailored biodistribution and new concept of targeting in drug delivery based on their shape dependent biorecognition.

Accordingly, in this study our concept for implementing a thermally switched two-way reversible shape memory in micrometer-sized spheres is an crosslinked network of a biocompatible star-shaped polymer, in which actuator domains (free PEG-PCL molecular chain) and shifting-geometry determining domains (the cross-linked PEG-PCL molecular chain) are co-exist. Currently, biodegradable shape-memory poly(ε-caprolactone)-co-poly(ethylene glycol) networks has been frequently adopted. [40, 41] This network is fabricated on the basis of well-defined six-arm poly(ethylene glycol)-poly(ε-caprolactone) (6A PEG-PCL) functionalized with vinyl end-groups and the predesigned architecture is easily achieved by photo crosslinking. For the polymer composition, PCL is frequently considered as an interesting material for potential shape memory applications in the biomedical field, due to its biodegradability. However, the high crystallinity reduces its compatibility with soft tissues and lowers its biodegradability.[42] Six-arm poly(ethylene glycol) (6A PEG) possesses excellent hydrophilicity and nontoxicity, and its copolymerization with ε-caprolactone monomers can overcome the drawbacks of PCL and reduce the transition temperature of shape memory close to body temperature. In contrast to other polymers with 2W SME, this polymer network is tailored for biomedical applications as reversibly changeable micrometer-sized carrier for drug delivery. To explore the SME on the micrometer scale, the spherical particles with average diameter of 5μm were prepared by an oil-in-water (o/w) emulsion technique. The particles with an ellipsoidal temporal shape were achieved by PVA film stretching at 60℃ with subsequent cooling to 0℃. The reversible shape memory recovery between spherical and ellipsoidal shape was realized with the cyclic heating and cooling between 43℃ and 0℃. In particular, macrophages were used as a model cell for the investigation of the internalization of these particles and subsequently intracellular shape memory recovery.

Experimental Section

Materials

ε-Caprolactone (ε-CL, 99.9%, Aldrich) were distilled over freshly powdered CaH_2 under a reduced pressure. 6-arm polyethylene glycol (6A PEG, Mn≈6000) was purchased from Liming Research Institute of Chemical Industry in Luoyang (China). Diphenyl (2,4,6-trimethylbenzoyl) phosphine oxide (TPO), stannous chloride (99%, $SnCl_2$) and polyvinyl alcohol (PVA 1788, average M.W. 88000, degree of hydrolysis %(mol/mol) 87.0～89.0) were purchased from Chengdu Kelong Chemical Reagent Company (China). Nile red was purchased from Adamas. All other chemicals and solvents were of reagent grade or better.

Fabrication of Chemically Crosslinked 6A PEG-PCL

6A PEG-PCL was firstly synthesized via ring-opening polymerization of ε-CL with 6A PEG as initiator in the presence of $SnCl_2$ as the catalyst.[43] A typical experimental procedure for the synthesis of the copolymers designated as 6A PEG-PCL is described as follows. Preweighed ε-CL, 6A PEG and $SnCl_2$ (1 wt%) were quickly added into a 50 mL bottom flask with a stopcock which was preheated to remove the moisture. Later, the reaction system was degassed under vacuum for 4h with continuous stirring to produce a well-mixed molten phase, and carried out at 140°C for 6 h. The obtained copolymer was firstly dissolved in dichloromethane. After suction filtration, the polymer solution precipitated in excess cold mixed liquid ($V_{ethyl\ alcohol}$:V_{H2O}=5:1). The 6A PEG-PCL in this mixture has been purified of residual oligomer and catalyst. To obtain the 6A PEG-PCL with vinyl end-groups (6A PEG-PCL-AC), acryloyl chloride was then reacted with the end of the chains of 6A PEG-PCL in the presence of triethylamine for removal of hydrogen chloride from the products ($M_{acryloyl\ chloride}$:$M_{triethylamine}$:$M_{6A\ PEG-PCL}$=6:6:1). Again, the obtained 6A PEG-PCL-AC was purified in excess cold mixed liquid (Vethyl alcohol:VH_2O=5:1) as 6A PEG-PCL. Later, preweighed 6A PEG-PCL-AC and 5 wt.% TPO were dissolved in CH_2Cl_2 under stirring to ensure uniform mixing. Then, the mixture was cast on a mold made of polytetrafluoroethylene (PTFE), and the mold was evaporated in aerator overnight and dried at room temperature (22 ℃). Finally, the completely dried 6A PEG-PCL-AC/TPO was kept in an oven at 60 ℃ to make it melt. Photo-crosslinking of 6-arm PEG-PCL-AC/TPO was initiated by the UV light (λ = 360 nm) generated from a high-intensity long wave UV lamp (100 W, intensity: 400 μW cm^{-2}) for 30 min.

Characterization

FT-IR was recorded on a Nicolet 5700IR spectrometer. All samples were obtained by KBr plates in which dry polymer power was mixed with KBr at a weight ratio of 0.5%~1%. The hydroxyl number were determined according to the Chinese National Standard GB 12008.3–89.The amount of reactive hydroxyl group on 6A PEG, 6A PEG-PCL and 6A PEG-PCLAC were measured by titration of excessive o-Phthalic anhydride groups. The molecular weights of 6A PEG ,6A PEG-PCL and 6A PEG-PCLAC were determined using For GPC (Waters 1515, USA) measurement, dimethylformamide

Journal of Materials Chemistry B Accepted Manuscript

This journal is © The Royal Society of Chemistry 2012

(DMF)/LiBr was used as the eluent at a flow rate of 1 mL/min at 40 ℃, and polymethyl methacrylate (PMMA) was used as reference. ^{1}H-NMR spectra were recorded with a Bruker AM-300 spectrometer. Tetramethylsilane (TMS) was used as the internal standard and $CDCl_3$ was used as solvent for 6A PEG-PCL, Differential scanning calorimetry (DSC) was employed to measure the thermal properties of polymers on a TA instrument (Q100, American). Nitrogen was used as purge gas with a flow rate of 20 mL min^{-1}, and the temperature increasing rate is 0.5℃ min^{-1}. Dynamic mechanical analysis (DMA) was carried out on a DMA983 analyzer (TA Instruments, America), using a tensile resonant mode at a heating rate of 5 ℃ min^{-1} from -10 to 60 ℃ and at a frequency of 1 Hz. Gel fraction estimate was performed according to the previous method.[44] In situ X-ray diffractometry (XRD) (Phlips, X'Pert PRO, Netherlands) was used to determine the crystallization property of crosslinked 6A PEG-PCL networks. The scanning range is 5–40°. These samples were heated from 25 ℃ to 60 ℃, then cooling to 0 ℃; In the second heating process, record the data when reaching each desired temperature and isotherm for 1 min. The water contact angle (CA) was measured using a sessile drop method at room temperature with the contact angle equipment (DSA 100, KRUSS, Germany).

Fabrication of Micrometer-Sized Particles

The spherical particles were fabricated with an oil-in-water (o/w) emulsion technique. Firstly, 0.25 g 6A PEG-PCL-AC and 0.0125 g TPO was dissolved in 8 mL CH_2Cl_2 with Nile red, a red-fluorescent dye that stained the polymer red. 0.5 g PVA was dissolved in 100 mL deionized water containing 100 μL Span-80 as surfactant, and the solution was used as emulsion stabilizer. The PEG-PCL-AC/TPO/Nile red mixed solution was added dropwise to the PVA solution using a disposable syringe (21 gauge) under mild stirring (200 r.p.m.) at room temperature. After the complete removal of organic solvent, in order to obtain a evenly distributed crosslinked micropaticles (microparticles will aggregate during centrifugation) the particles were also photo-crosslinked as described above. Finally, the resultant particles were rinsed five times with distilled water and collected by centrifugation.

Spherical Particles Programming to Their Temporary Shapes

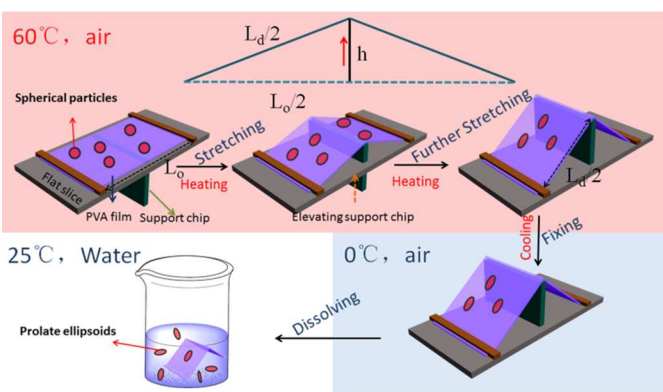

Scheme 1. Spherical particles programming to their temporary shapes.

The shape changeable particles were fabricated using a modified PVA film stretching method as illustrated in **Scheme. 1**. Firstly, the spherical particles (0.3 wt.%) were dispersed into 5ml 5% PVA water solution at 22 ℃ including 2% glycerol as plasticizer for the resultant PVA film, and the mixed solution was poured in a mold with a size of 10 ×10 cm (length × width) and dried at room temperature to acquire PVA film with a thicknesses of 200 μm. Secondly, the PVA film was typically cut into sections of 10 ×5 cm and pasted on the metal plate. In cases of heat-stretching, the film was heated in 60 ℃ for 10 min and then the preset support chip was inserted into the slot. The spherical particles inside PVA film were stretched to ellipsoids with different aspect ratios (AR) by controlling the degree of tensile of the film which was in proportion to the height of elevated support chip. Finally, the metal plate and the deformed film was cooled in 0 ℃ for 30 min to fix the ellipsoidal temporal shape. The film was dissolved in water at 25 ℃. The ellipsoids were collected by centrifugation and rinsed 5 times with distilled water to remove all PVA from the surface of the particles. The particle size and distribution were determined with laser diffraction particle size analyzer ((LA-9200, HORIBA, Japan). The morphology was observed with confocal laser scanning microscopy (CLSM, FV1000, Olympus, Japan).

Macroscopic and Microcosmic Reversible Shape Memory Effect

Reversible shape memory cycle was performed under a typical investigation procedure.[45] Samples were thermally equilibrated on a DMA983 analyzer at 60 ℃ for 1 min before the data were recorded. Stress was then increased from 0 to 0.5 MPa at a rate of 0.01 MPa per second and fixed at 0.5 MPa while temperature cooled to 0 ℃ at a rate of 5 ℃ per minute. The temperature was equilibrated at 0 ℃ for 1 min, then stress isothermally unloaded back to 0 MPa at a rate of 0.01 MPa per second. Finally, free-strain cyclic recovery was measured with the cyclic heating and cooling between 43℃ and 0℃. The macroscopic shape memory effect in the initial shape of ribbon-like were firstly investigated by a heating from 30 ℃ to 37 ℃, 39 ℃, and 42 ℃, respectively. The reversible shape memory recovery processes in form of both ribbon and micro-sized sphere were investigated at an alternant temperature between 0 ℃ and 43 ℃ according to the DMA result. After 30 min, the system reached an equilibrium for each temperature change during the shape memory cycles.

In Vitro Cytotoxicity Assay

The cytotoxicity of all the samples was further evaluated based on Alamar blue assay.[46] Firstly, c-6A PCL and c-6A PEG-PCL were sterilized by UV for 4 h. The UV wavelength was 365 nm, and the power of this UV lamp is 12W. These samples were cut into small round flakes with average diameters of nearly 12 mm for all the samples, and then they were used for osteoblasts culture in vitro. The cells belonged to normal cell line, which were from neonatal rat's mandibular. They have been passaged to the third generation just before our experiments. In brief, the osteoblasts cells were grown in RPMI medium 1640 (Gibcos) with 10% fetal bovine serum (FBS). The cells with a density of 1.0 × 10^4 cells/well were cultured in 24 well plates in the above medium and maintained at 37 ℃ in a humidified incubator with 5% CO_2 and 95% air. At pre-designed time points of 1, 3, 5 days, medium was carefully removed and 300 μL Alamar blue solutions (10% Alamar blue, 80% media 199 (Gibcos) and 10% FBS; V/V) were added to each well and incubated for further 3 h at 37℃, 5% CO_2. Wells without cells were used as the blank controls. A sample of 200 μL of reduced Alamar blue solution was pipetted into costar opaque black bottom 96-well plate (Sigma)

Journal of Materials Chemistry B Accepted Manuscript

and read at 570 (excitation)/600 (emission) in a ELISA microplate reader (Molecular Devices, Sunnyvale, CA). Results were the mean ± standard deviation of three experiments. Cell morphology and growth on the surfaces of the meshes were evaluated by fluorescence microscopy (IX51,Olympus, Japan).

Phagocytosis and Intracellular Shape Memory Recovery

The mouse macrophage cell lines as model macrophages were obtained from the Sichuan University (China). They were cultured in DMEM media containing L-glutamine and 10% fetal bovine serum (FBS). The macrophages cells were grown in 6-well tissue culture-treated slides (BD Biosciences) at a concentration of 1×10^5 cells/mL, incubated at 37℃ for 24 h. Non-attached cells were removed by aspiration, later, 200 μL of fresh media containing 1 mg spherical or ellipsoidal micro-sized particles was added in the 6-cell culture plate and co-cultured with macrophages for 5, 15, 30 and 60 min at 37 ℃. For investigation of intracellular shape memory recovery, after the

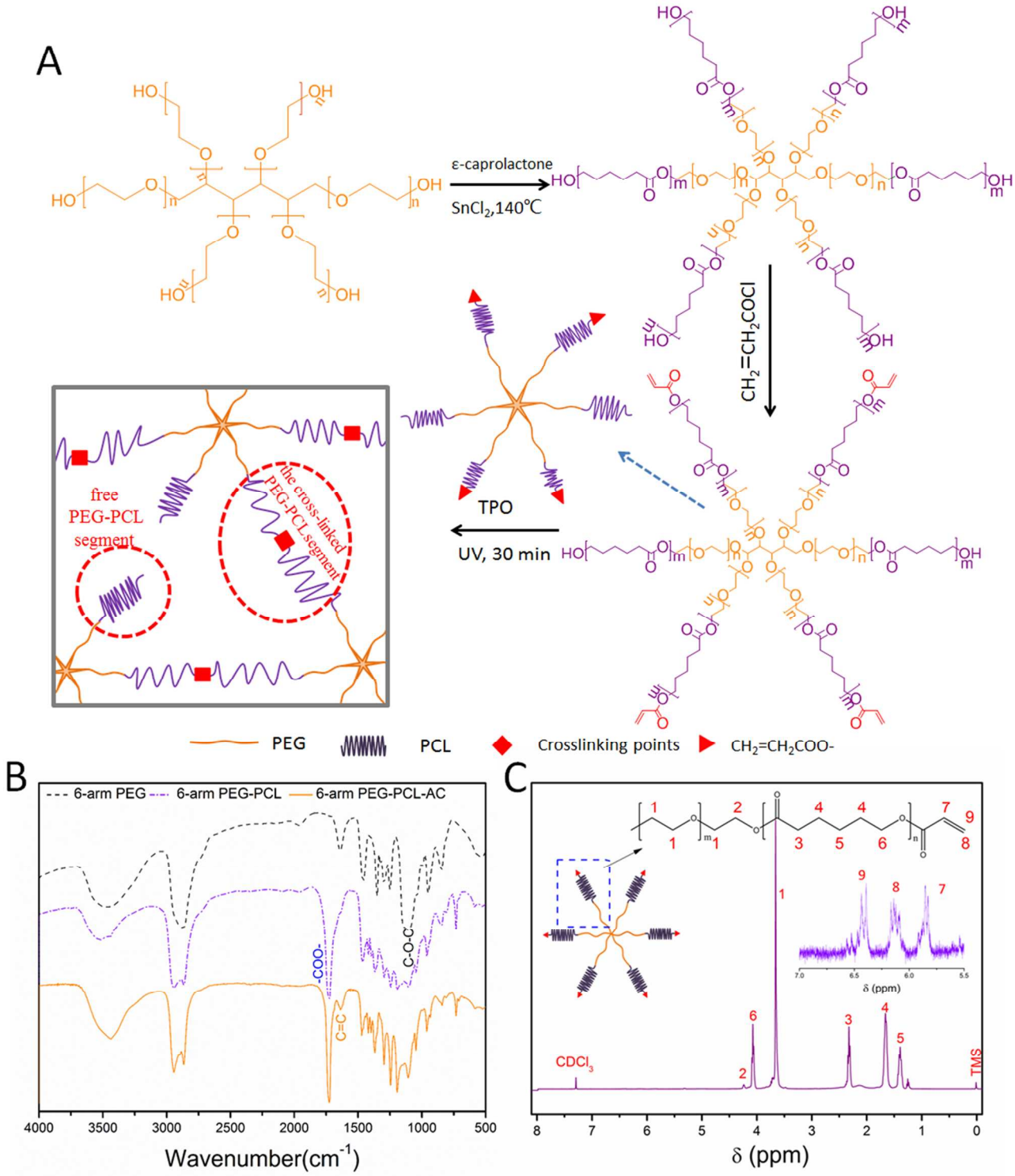

Fig. 1. Synthesis and thermal properties of the crosslinked network based on c-6A PEG-CL. (A) Scheme of the synthesis of c-6A PEG-PCL network, (B) FT-IR spectra of 6-PEG, 6A PEG-PCL and 6A PEG-PCL-AC, (C) 1H NMR of 6A PEG-PCL-AC.

Journal of Materials Chemistry B Accepted Manuscript

cells treated with ellipsoidal particles for 30 min at 37 ℃, these cells underwent cyclic heating and cooling between 43 ℃ and 0 ℃. Finally the cells were fixed with 2.5% glutaraldehyde, washed with PBS. Images were acquired on a CLSM (FV1000, Olympus, Japan).

Results and discussions

Characterization of c-6A PEG-PCL

The crosslinked network on the basis of chemically crosslinked six-arm poly(ethylene glycol)-poly(ε-caprolactone) (c-6A PEG-PCL) was achieved as schematically shown in Fig. 1A. From the FT-IR spectrum of 6A PEG-PCL (Fig. 1B), we can find that the characteristic peak of C-O-C at 1125 cm^{-1} belongs to PEG chains, the peak at 1730 cm^{-1} is related to O=C-O, indicating the successful ring-opening polymerization of ε-CL. The appearance of the peak at 1640 cm^{-1} from the spectrum of 6A PEG-PCL-AC suggested that the acryloyl chloride did react with the terminal hydroxy of 6A PEG-PCL, which is the characteristic stretching vibration absorption peak of C=C. The amount of hydroxyl group on 6A PEG and 6A PEG-PCL was 54±3.2 mg KOH/g and 17.3±2.4 mg KOH/g, respectively. After grafting acryloyl chloride, the amount of hydroxyl group on 6A PEG-PCL was 3±1.2 mg KOH/g, indicating that the grafting ratio was 79±3%. In order to further confirm the results from hydroxyl number, GPC measurements for these polymer were performed and the results were shown in Table S1 in SI. Remarkably, the grafting ratio of acryloyl chloride and the molecular weight of PCL segments exert an effect on the structure of the c-6A PEG-PCL, and the gel fraction should be proportional to grafting ratio and the crosslinking time. In this polymer network, we may regulate the content of acryloyl chloride in grafting reaction and the crosslinking time to control the proportion of the cross-linked PEG-PCL molecule chains and free PEG-PCL molecular chains.

Intermolecular transesterification reactions modify the sequences of copolylactones and prevent the formation of block copolymers. The types of intermolecular transesterification reactions broaden the molecular weight distribution. Due to these side reactions MWDs of the polymers are above 1.3 and the product is a mixture of both linear and cyclic molecules.[47-49] GPC measurements have shown that both linear or microgel could not be detected in the polymerization mixtures up to the monomer conversion approaching 99.9%. Thus, if any both linear oligomers would be present in the system, they

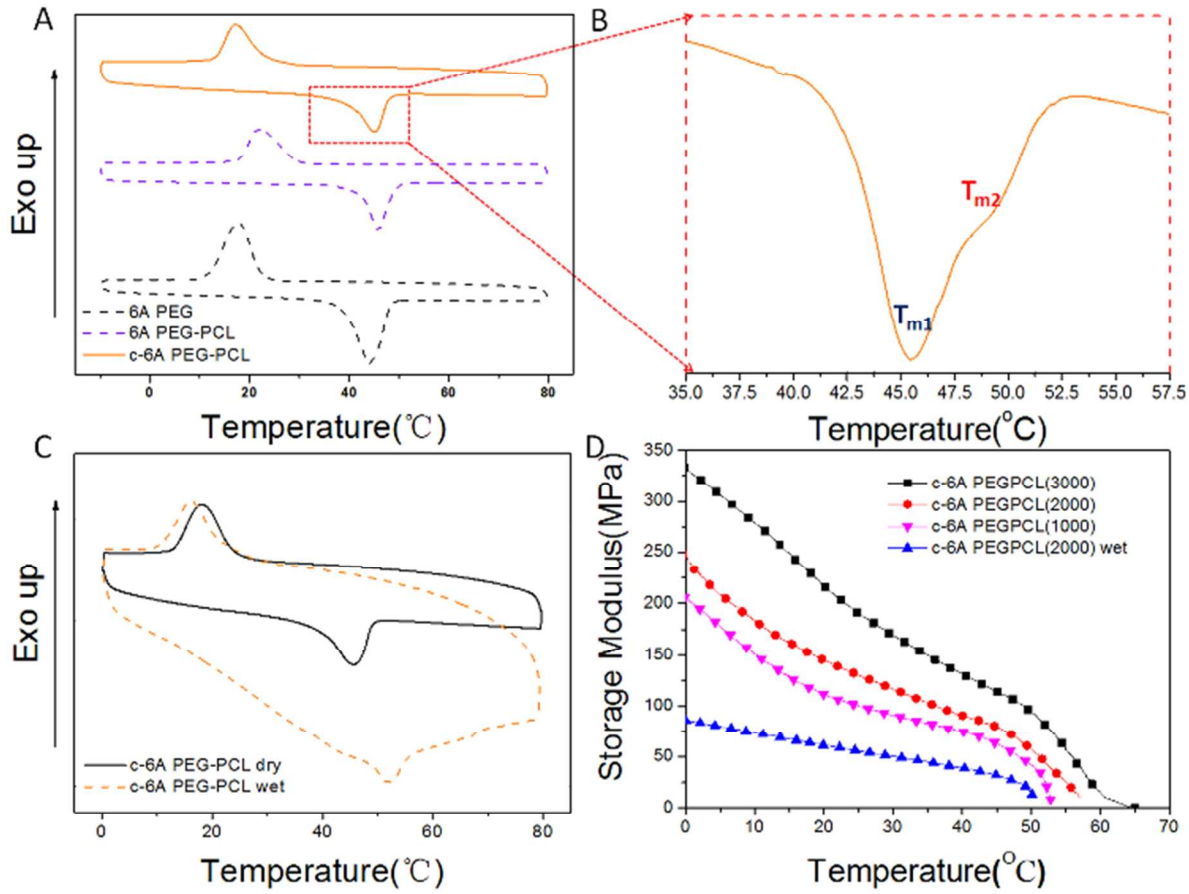

Fig. 2 **(A)** DSC curves of 6A PEG, 6A-PEG-PCL and c-6A PEG-PCL(2000), **(B)** is a magnified view of c-6A PEG-PCL, **(C)** DSC curves of c-6A PEG-PCL under dry and wet conditions, **(D)** DMA curves of storage modulus of c-6A PEG-PCL polymers with the M_w of each PCL arm of 1000 g mol^{-1}, 2000 g mol^{-1} and 3000 g mol^{-1} and c-6A PEG-PCL(2000) under wet condition, respectively.

Journal of Materials Chemistry B Accepted Manuscript

should constitute less than 0.1% of the linear polymer.

To further confirm that 6A PEG-PCL-AC was synthesized successfully, the structure was verified by ^{1}H-NMR as shown in in **Fig. 1C**. In the ^{1}H NMR spectrum, the peak around 3.55 ppm is attributed to the methylene hydrogen atoms (-CH_2-O-) of the PEG blocks. The peaks at 2.25, 1.57, 1.32 and 4.02 ppm are all assigned to the methylene hydrogen atoms (-CH_2-CH_2-CH_2-CH_2-CH_2-) of PCL units. ^{1}H NMR was used to determine the number of monomer units in each block, and the average repeated unit number of CL is assigned to the carbon-carbon double bond hydrogen atoms (-CH=CH-) located in the end of the polymer chains. The grafting ratio of carbon-carbon double bond was also determined from the area ratio of the ^{1}H NMR peaks at 5.8 ppm (owing to the acryloyl chloride blocks), and 4.1 ppm (owing to the PEG blocks), the value was calculated to be 77%. The melting behavior of c-6A PEG-PCL with different molecular weight (M_w) of PCL was investigated using DSC analysis, as shown in q in the Support Information (SI). From the curves, we can find that with the M_w of each PCL arm increasing from 1000 g mol^{-1} to 2000 g mol^{-1} and 3000 g mol^{-1}, the T_m increase

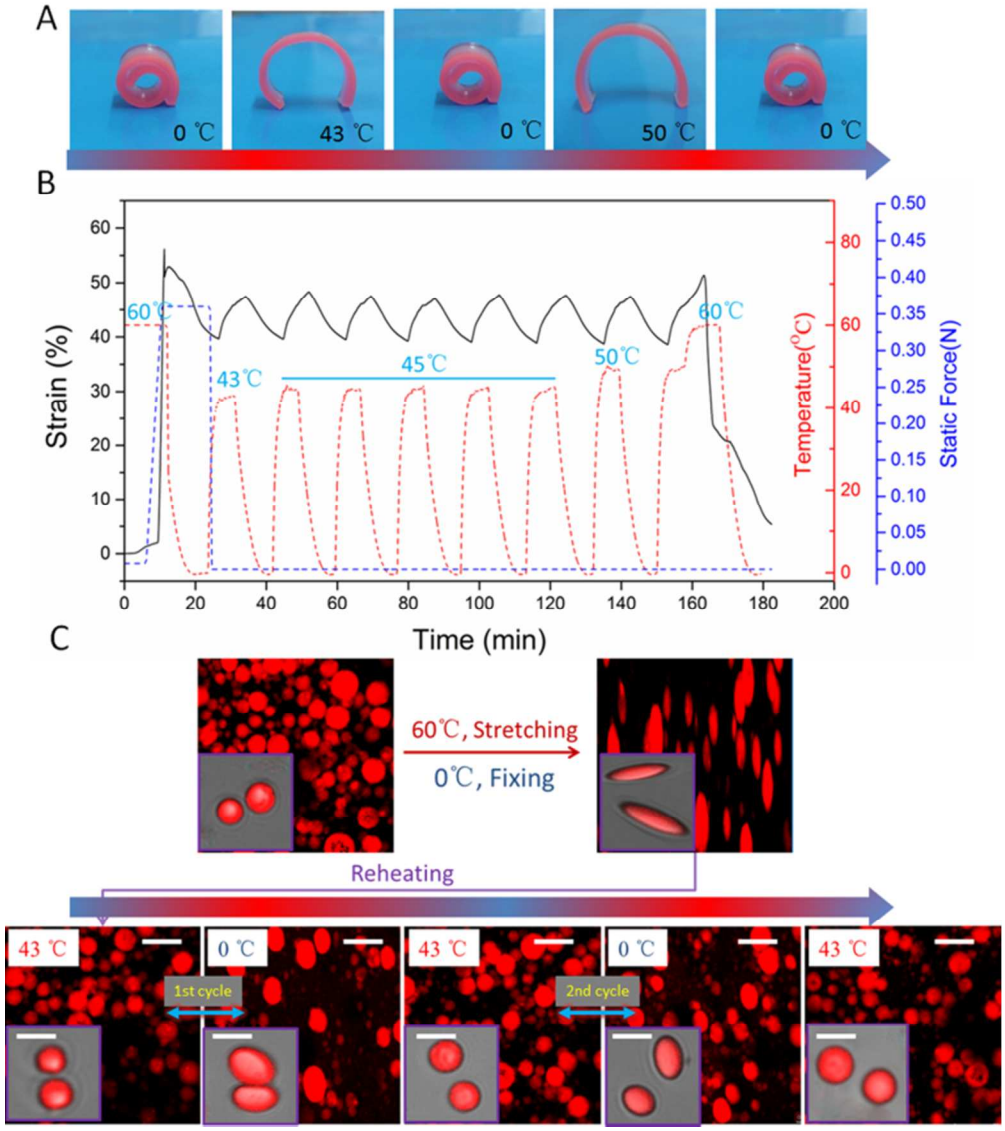

Fig. 3 The reversible shape memory recovery behaviors of c-6A PEG-PCL(2000). (A) Series of photographs macroscopically showing the reversible shape memory recovery process. (B) Consecutive reversible SME. (C) Fluorescence images showing the deformation and fixation of the micro-sized particles (the stretching strain of PVA film≈200%), and microscopically reversible shape memory recovery process of the particles. The insert images are obtained by CLSM (Scale bar: 10μm).

19 in the 6A-PEG-PCL polymer. Here we can find three additional weak peaks at 5.8, 6.2 and 6.4 ppm in the close-up image, they are from 35℃ to 41℃ and 51℃, respectively. In contrast to the influence of the crosslinking on the thermal properties, we can see

Journal of Materials Chemistry B Accepted Manuscript

This journal is © The Royal Society of Chemistry 2012

that the crosslinking make the T_m decrease slightly (Fig. 2A). The uncross-linked polymer shows the higher values of melting temperatures than the crosslinked networks. The T_m of c-6A PEG-PCL(2000) is close to the physiological temperature, which is very suitable for acting as thermally induced SMP for biomedical applications. Actually the T_m of c-6A PEG-PCL(1000) is closer to it, but it is lower. Considering the clinical application, we hope that it will be a little higher than the physiological temperature, thus we have enough time to carry out the shape memory recovery process at the critical point. Consequently, all of the following investigations are focused on c-6A PEG-PCL(2000). The further amplification of the melting peak of c-6A PEG-PCL(2000) is shown in Fig. 2B, and we can find that two endothermic peaks appear in the DSC curve, demonstrating that phase separation took place in the polymer network to form crosslinking part (the previous peak) and free segment (the second peak). The higher crystallinity with higher T_{m2} is ascribed to the free PEG-PCL segment, and the lower one with lower T_{m1} is for the cross-linked PEG-PCL of this crosslinked network as shown in Fig. 1A. Since the material would be potentially used as biomaterial and it would contact water in the body, the effect of water on thermal property was further investigated. Fig. 2C displays the DSC curves of c-6A PEG-PCL under dry and wet conditions respectively. After c-6A PEG-PCL was immersed in water for 1 h, the water content in the polymer network is 15.34 wt.%, determined by thermal gravimetric analysis (TGA) (Fig. S2 in SI). In Fig. 2C we can find that the H_2O molecules penetrating into polymer network lead the melting transition region to turning broad, suggesting that the aqueous environment brings an impact on the crystallization of this polymer. This broad melting transition region can endow the polymer a temperature memory function. [50-52]

Macroscopic Reversible Shape Memory Effect

Dynamic mechanical analysis (DMA) was performed for polymer to predict shape memory property. Fig. 2D shows the DMA curves of c-6A PEG-PCL networks with different molecular weights for each PCL arm under dry condition and c-6A PEG-PCL (2000) under wet condition. All of these polymers display a systematical decrease in the storage modulus (E') with increasing temperature. The decrease of molecular weight of PCL brings a decrease in the transition temperature (T_{trans}) of c-6A PEG-PCL, which is in good agreement with the DSC analysis. Additionally, the E' values of all specimens firstly experienced a platform over 100 MPa at low temperature, and then dropped to a new modulus plain of about 0.01 MPa at high temperature.The tremendous change in E' has been proven to have an obvious contribution to a good shape-memory effect.[53] Compared the DMA curves of c-6A PEG-PCL(2000) under dry and wet conditions, it can be seen that there are more gaps in E′, which can be essentially attributed to the plasticizing effect of H_2O.[54] Moreover, the polymer having a relatively broad transition temperature range suggests that it maybe has a good multiple shape memory effect.[55, 56]

According to above DMA analysis, the temperature in the range of 30~43 ℃ can be selected as the shape recovery temperature. To demonstrate that the c-6A PEG-PCL has good SME, Fig. S3 in SI gives series of photos of the macroscopic multiple shape-recovery process and temperature memory effect of the c-6A PEG-PCL(2000) at 0 ℃, 37 ℃, 42 ℃ and 45 ℃. It can be observed that the c-6A PEG-PCL possesses a multiple shape memory effect in the temperature range of 30~43 ℃. Furthermore, we found that the c-6A PEG-PCL have temperature memory effect with different deformation temperature. After deformation above 45 ℃, the shape recovery can't happen at body temperature. These result shows that the T_{trans} and shape recovery ratio can controlled by the deformation temperature in a real application such as intravascular stent and drug carrier.

As shown in Fig. 3A and Movie S1 in SI, the c-6A PEG-PCL ribbon is programmed to form a ring shape at 60 ℃, cooling to 0 ℃ for fixation of this shape, and subsequent heating to 43 ℃ again. Cooling back to 0 ℃ results in the shape of hovering. Cyclic heating and cooling between 43 ℃ and 0 ℃ reversibly switches between ring shape and arch shape. Heating to 60 ℃ erases shapes "ring" and "arch" from the memory of the polymer due to the fact that all crystalline domains were melt. The effect of crosslinking degree derived from crosslinking time on SME was also studied (Fig. S4 in SI). We find that the polymer has excellent reversible SME when the gel fraction is in the range of 68%~81%.

To further demonstrate that this polymer had good reversible SME, a cyclic tensile test was carried out. Fig. 3B shows the typical strain-stress curves versus temperature change. Firstly, the c-6A PEG-PCL is immersed in 60 ℃ H_2O bath for 1 h before test, as the c-6A PEG-PCL can be potentially used in body fluid as biomaterials. Then, the samples were thermally equilibrated at 60 ℃ for 1 min before the data were recorded. Stress was then increased from 0 to 0.5 MPa at a rate of 0.05 MPa per second and fixed at 0.5 MPa while temperature cooled to 0 ℃ at a rate of 5 ℃ min^{-1}. The temperature was equilibrated at 0 ℃ for 1 min, then stress isothermally unloaded back to 0 MPa at a rate of 0.5 MPa per second (the shape fixity ratio of c-6A PEG-PCL remained over 90% (91.7%)). Then the temperature was increased to 43 ℃ at a rate of 5 ℃ min^{-1}. Finally the shape memory recovery was realized with the cyclic heating and cooling between 45 ℃ and 0 ℃. In Fig. 3B, the strain ε is plotted against time for the first reversibility cycle. We can find that the changes of ε is spontaneous, without action of external force beginning from the second cycle. In the following alternant cycles, the sample switched reversibly between elongate shapes and half recovered shape. After seven cycles, the temperature rises to 60 ℃, the piece returns to its original shape. Cooling back to 0 ℃ again, the reversible shape memory effect could not occur, it is mainly because of the molecular chains of c-6A PEG-PCL became amorphous and subsequently the reversible shape memory effect disappeared.

Microscopic Reversible Shape Memory Effect

To explore the microscopic reversible shape memory effect, this polymer was fabricated to spherical micrometer-sized particles with an average size of 5 μm (Fig. S5 in SI). These spherical particles (permanent shape) are programmed to ellipsoids (temporal shape) through a modified PVA film-stretching technique as shown in Scheme 1. By changing the stretching strain (height of support chip), the ellipsoids with different aspect ratios (AR) from 1 to 5 can be easily achieved. From Fig. S5, we find that the particle size and

Journal of Materials Chemistry B Accepted Manuscript

distribution of the deformed particles are almost similar with original particles due to the fact that the volume of particle is not changed. The effect of stretching strength or degree of tensile on particle shape (AR ratio) as shown in Fig. S6 in SI. To clearly observe the morphology and the shape memory process of these particles, they were stained with fluorescent dye, Nile red. From the CLSM images in Fig. 3C, we can see that the particles take on a well-spherical shape inside PVA film and turn to prolate ellipsoids after they were stretched at 60 ℃ and immediately cooled at 0 ℃. These particles were collected by dissolving PVA film in water. The microscopic reversible shape memory effect was also observed by CLSM (Fig. 3C), it can be seen that the particles are capable of switching their shape reversibly from spherical to ellipsoidal with the cyclic heating and cooling between 43 ℃ and 0 ℃.

The Mechanism of Reversible Shape Memory Effect

From above discussion, we know that this polymer network possess obvious reversible shape memory effect. To analyze the relationship between the structure of this polymer and reversible SME, in-situ temperature X-ray diffraction (XRD) and small-angle X-ray scattering (SAXS) was carried out. Fig. 4A and B show the XRD patterns of c-6A PEG-PCL film under dry and wet conditions

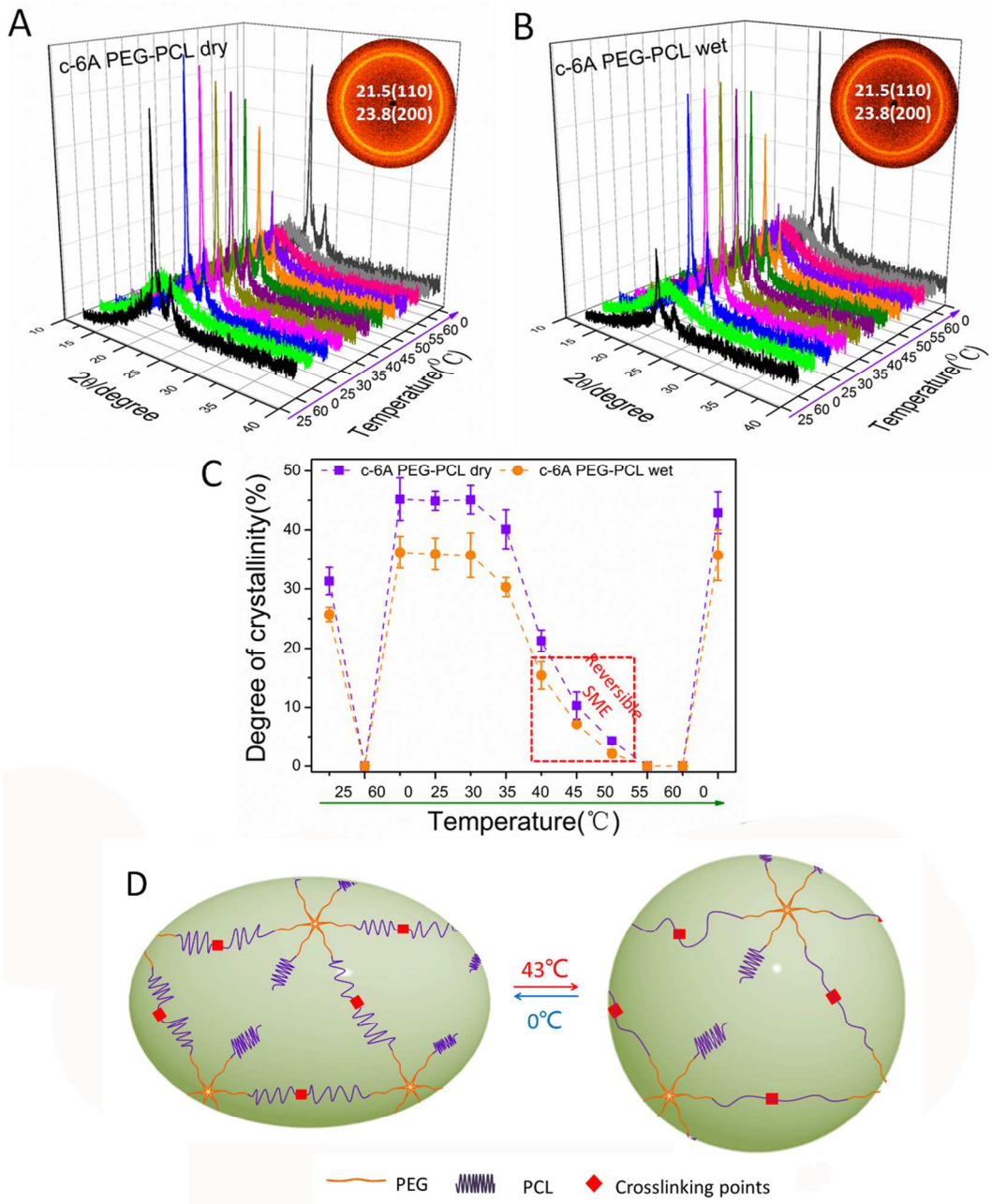

Figure 4. The relationship between the structure of the polymer and reversible SME. **(A)**, **(B)** in-situ temperature XRD patterns of c-6A PEG-PCL(2000) under dry and wet conditions respectively. The inserts are the diffraction rings acquired from SAXS (the SAXS data measured at t~4,100 s). **(C)** The crystallinity under dry and wet conditions versus determined temperatures. **(D)** The schematically molecular mechanism of the thermally induced reversible SME.

Journal of Materials Chemistry B Accepted Manuscript

This journal is © The Royal Society of Chemistry 2012

respectively. The water penetrating into this polymer film leads the degree of crystallization at a same temperature to decreasing, which is also consistent with DSC analysis. The crystalline peaks at 2θ =21.5° (110) and 23.8° (200) are ascribed to the PCL segments, confirming its semi-crystalline structure. While for all temperature, there exit no obvious characteristic peaks corresponding to PEG (19.24° and 23.42°). With the temperature rising above 40 ℃, the crystallization behavior of PCL became worse. Under the wet condition, the degree of crystallization decreased from about 30% at 0℃ to 7% at 43 ℃ (Fig. 4C). Remarkably, after the temperature was raised to 60 ℃, the molecular chains of c-6A PEG-PCL became amorphous and subsequently the reversible shape memory effect disappeared.

The molecular mechanism of the thermally induced reversible shape memory effect of the c-6A PEG-PCL microsphere is schematically illustrated in Fig. 4D. In one-way SMPs, the switching domains provide two functions at the same time. They enable active movement from the temporary shape B to the original shape A by elastic recovery and determine the geometry of the shape change by temporary fixation of shape B.[57] In chemical structure of one-way shape memory polymer, there lacks actuator domains (ADs) which are capable of driving permanent shape to return to temporal shape upon cooling. In order to indicated the exact mechanism, the shape memory effect of c-6A PEG-PCL with different ratio of 6A PEG-PCL to 6A PEG-PCL-AC was carried out. To ensure that the c-6A PEG-PCL was completely cross-linked, photo-crosslinking of 6A PEG-PCL/6-arm PEG-PCL-AC/TPO was initiated by the UV light for 40 min. Fig. S8 shows the gel fraction, shape fixed ratio and shape recovery ratio with different ratio of 6A PEG-PCL to 6A PEG-PCL-AC. We can find that 6A PEG-PCL-AC was cross-linked with each other under the UV light. In addition, as the content of 6A PEG-PCL-AC increased, shape fixed ratio and shape recovery ratio of c-6A PEG-PCL increased. More specially, only the samples of 30:70 and 20:80 (6A PEG-PCL/6A PEG-PCL-AC) shows reversible shape memory effect. And here it becomes evident, in this polymer network, there exist two different units: the cross-linked PEG-PCL molecule chains and free PEG-PCL molecular chain. The crosslinked PCL regions with lower melting temperature ($T_{m,AD}$) acting as actuator domains (ADs) are responsible for the actuation of the 2W SME, and the free PCL segments determine the shape shifting geometry due to the higher $T_{m,SGD}$. Thus, a temperature-responsive "on–off" crystallinity transition from the reversible crystallization and melting of oriented ADs can be achieved under a stress-free condition, and subsequently the 2W SME is realized. During the reversible shape memory recovery process, the free PEG-PCL molecular chain can perform a skeletons role and induce or regulate the shape change of the cross-linked 6-arm molecules. [32, 37]

Cytotoxicity Analysis

The cytotoxicity of 6A PEG-PCL and its degradation products was assessed with Alamar blue assay. The hydrophobic 6A PCL is selected as control, which was synthesized by the initiating of dipentaerythritol. The hydrophilicity of PCL was greatly improved

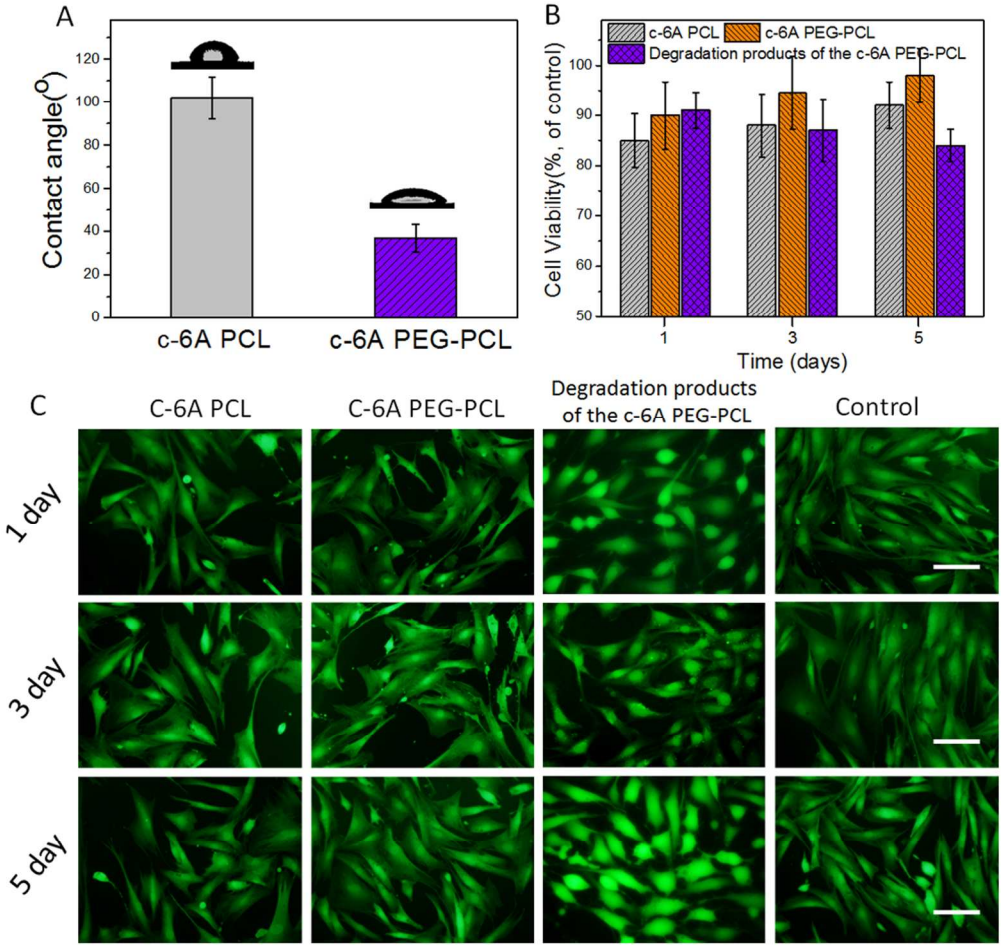

Fig. 5. Evaluation of in vitro cytotoxicity. **(A)** Analysis of water contact angle of c-6A PCL and c-6A PEG-PCL. (B) Cell viability and (C) fluorescence microscope images of osteoblasts cultured on c-6A PCL and c-6A PEG-PCL at day 1, day 3 and day 5, respectively. The live cells were stained green with calcein. (Scale bar: 10μm)

Journal of Materials Chemistry B Accepted Manuscript

with the introduction of 6A PEG (Fig. 5A). Fig. 5B,C show the cell viability and representative fluorescence microscope images of osteoblasts treated the 6A PCL, 6A PEG-PCL and the degradation products of the 6A PEG-PCL, respectively. We can find that more than 85% of the cells remained viable, and the cell viability of 6A PEG-PCL is better than that of 6A PCL due to the improvement of the hydrophilicity. From Fig. 5C, it could be clearly found that the obsteoblasts was elongated but attached and spread well on polymer substrates. Moreover, obsteoblasts cells were incubated with the degradation products (6-hydroxycaproic acid and its oligomers and 6A PEG) for various incubation times. In Fig.5B, it can be obviously observed that all of the cell viability for degradation products at the 1st day, 3rd day and 5th day was more than 80%. Cells' shape was also completely spread out, indicating that their growth is healthy. All these results strongly proved that the c-6A PEG-PCL has excellent cytocompatibility, suggesting that it is very suitable for biomedical applications.

Phagocytosis and Subsequently Intracellular Shape Memory Recovery

Particle shape has an impact on phagocytic internalization.[5-8] Internalization of the spherical and ellipsoidal micro-sized particles by macrophages was further observed with CLSM. The ellipsoidal particles with AR of 5 could not be taken up by macrophages (data not shown). The images shown in Fig. 6A exhibit that the phagocytosis has a strong dependence on local particle shape. In 5 minutes, both the spherical and ellipsoidal particles with AR of 1.6 are attached to the macrophage membrane, and the ellipsoidal particles associate with the membrane along the major axis of these particles. After 15 minutes, we captured that the whole spherical particles were taken up, while the ellipsoidal particle still stayed on the membrane. After 60 minutes, 15% spherical particles (5-10 um) were internalized by the macrophages, whereas only 3% ellipsoidal particles were swallowed, the main reason is that the size of particles is too large (Fig. S9). It is not hard to find that particles with high AR own the potential to inhibit phagocytosis. The result is consistent with previous report.[5] So the phagocytic fate of the particles depends largely on the polarizability. Thus, the ellipsoidal particles used as drug carrier will prolong blood circulation because they can evade phagocytosis by macrophages during delivery. Once the deformed particles arrive in target tissues, they can recover to spherical particles through a mild stimulus and in turn be facilely internalized by targeting cells. By adjusting the aspect ratio (AR) of the shape-switching particles, we can easily control the particles as drug delivery carriers to either avoid or promote phagocytosis.

Subsequently, the intracellular shape memory recovery was further investigated. From the fluorescence microscopy images (Fig. 6B), we can clearly see that after the ellipsoidal particles with AR of 1.6 was swallowed into macrophages, the morphology of the particles still can switch alternatively from the spherical to ellipsoidal shape between 43 and 0 ℃. This process is just like it of extracellular experiment. The intracellular environment won't make a difference to the Reversible shape memory behavior. After particles enter into cell, they will go on encountering these compartments inside cell, namely early endosomes, late endosomes and lysosomes. The intracellularly reversible shape memory recovery may open up a strategy towards investigating the intracellular behaviors of the carriers such as intracellular drug release, the interaction between carriers and compartments and nuclear drug delivery.

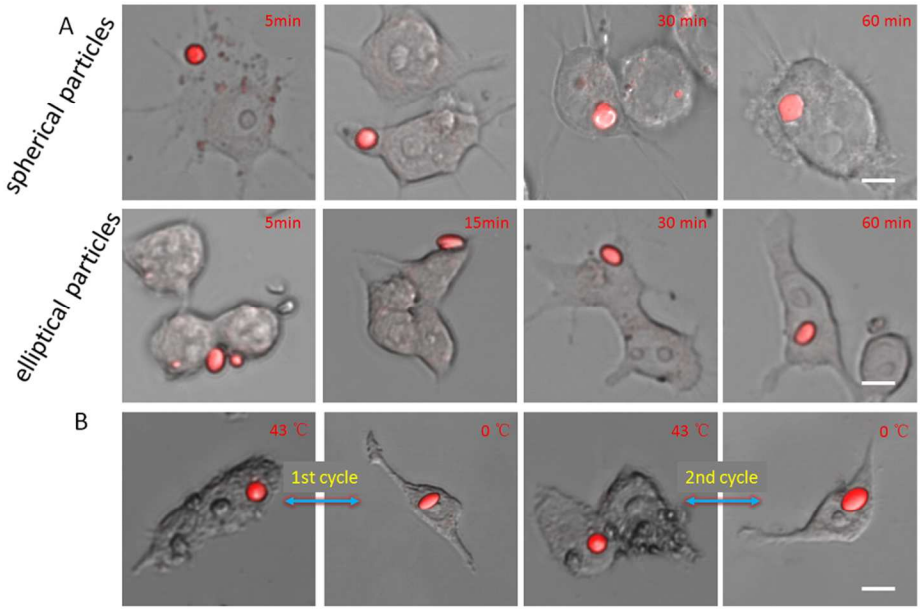

Fig. 6 Phagocytosis and intracellular shape memory recovery of the shape-switching particles. (A) The association process of both spherical and ellipsoidal particles with macrophages, observed with CLSM at 5 min, 15 min, 30 min and 60 min. These particles are stained with fluorescent dye, Nile red. (B) Confocal images showing the intracellularly reversible shape memory recovery of the particles. (Scale bar: 10μm).

Conclusions

Journal of Materials Chemistry B Accepted Manuscript

This journal is © The Royal Society of Chemistry 2012

In summary, we have originally developed one type of shape-switchable micrometer-sized particles based on a crosslinked polymer network including biocompatible six-arm poly(ethylene glycol)-poly(ε-caprolactone). These particles have an ability of reversibly switching their shape both extracellularly and intracellularly with the cyclic heating and cooling between 43 ℃ and 0 ℃ via the reversible 2W SME of polymer matrix. The molecular mechanism of the 2W SME can be ascribed to a temperature-responsive "on–off" crystallinity transition from the reversible crystallization and melting. By adjusting the aspect ratio (AR) of the shape-switching particles, we can control the particles as drug delivery carriers to either avoid or promote phagocytosis. Therefore, the study provides a new concept of dynamically shape-switching carriers in drug delivery.

Acknowledgements

This work was partially supported by National Basic Research Program of China (973 Program, 2012CB933600), National Natural Science Foundation of China (Nos.30970723, 51173150, 51373138) and Research Fund for the Doctoral Program of Higher Education of China (20120184110029). T Gong and K Zhao contributed equally to this work.

Supporting Information

Electronic Supplementary Information (ESI) available:

Notes and references

Key Laboratory of Advanced Technologies of Materials, Ministry of Education, School of Materials Science and Engineering, Southwest Jiaotong University, Chengdu, 610031, P. R. China. E-mail: shaobingzhou@swjtu.cn; shaobingzhou@hotmail.com

1. R. Duncan,*Nat. Rev. Drug Discov.*, 2003, **2**, 347-360.
2. J. M. Karp and R. Langer,*Curr. Opin. Biotech.*, 2007, **18**, 454-459.
3. D. Peer, J. M. Karp, S. Hong, O. C. Farokhzad, R. Margalit and R. Langer,*Nat. Nanotechnol.*, 2007, **2**, 751-760.
4. N. Doshi and S. Mitragotri,*Adv. Funct. Mater.*, 2009, **19**, 3843-3854.
5. J. A. Champion and S. Mitragotri,*Proc. Natl. Acad. Sci. USA*, 2006, **103**, 4930-4934.
6. S. E. Gratton, P. A. Ropp, P. D. Pohlhaus, J. C. Luft, V. J. Madden, M. E. Napier and J. M. DeSimone,*Proc. Natl. Acad. Sci. USA*, 2008, **105**, 11613-11618.
7. X. Hu, J. Hu, J. Tian, Z. Ge, G. Zhang, K. Luo and S. Liu,*J. Am. Chem. Soc.*, 2013, **135**, 17617-17629.
8. X. Huang, X. Teng, D. Chen, F. Tang and J. He,*Biomaterials*, 2010, **31**, 438-448.
9. S. Muro, C. Garnacho, J. A. Champion, J. Leferovich, C. Gajewski, E. H. Schuchman, S. Mitragotri and V. R. Muzykantov,*Mol. Ther.*, 2008, **16**, 1450-1458.
10. T. Chen, X. Guo, X. Liu, S. Shi, J. Wang, C. Shi, Z. Qian and S. Zhou,*Adv. Healthc. Mater.*, 2012, **1**, 214-224.
11. Y. Geng, P. Dalhaimer, S. Cai, R. Tsai, M. Tewari, T. Minko and D. E. Discher, *Nat. Nanotechnol.*, 2007, **2**, 249-255.
12. H. Meng, S. Yang, Z. Li, T. Xia, J. Chen, Z. Ji, H. Zhang, X. Wang, S. Lin and C. Huang,*ACS nano*, 2011, **5**, 4434-4447.
13. N. Doshi, B. Prabhakarpandian, A. Rea-Ramsey, K. Pant, S. Sundaram and S. Mitragotri,*J.Control. Release*, 2010, **146**, 196-200.
14. L. E. Euliss, J. A. DuPont, S. Gratton and J. DeSimone,*Chem. Soc. Rev.*, 2006, **35**, 1095-1104.
15. J. A. Champion, Y. K. Katare and S. Mitragotri, Particle shape: a new design parameter for micro-and nanoscale drug delivery carriers,*J. Control. Release*, 2007, **121**, 3-9.
16. M. R. Langille, M. L. Personick, J. Zhang and C. A. Mirkin,*J. Am. Chem. Soc.*, 2011, **133**, 10414-10417.
17. T. J. Merkel, K. P. Herlihy, J. Nunes, R. M. Orgel, J. P. Rolland and J. M. DeSimone, Scalable,*Langmuir*, 2009, **26**, 13086-13096.
18. S. Chen, J. G. Bomer, W. G. van der Wiel, E. T. Carlen and A. van den Berg, *ACS Nano*, 2009, **3**, 3485-3492.
19. C. Wischke, M. Schossig and A. Lendlein,*Small*, 2014, **10**, 83-87.
20. C. Wischke and A. Lendlein,*Langmuir*, 2014, **30**, 2820-2827.
21. T. Wu, K. O'Kelly and B. Chen,*Eur. Polym. J.*, 2014, **53**, 230-237.
22. A. Lendlein and S. Kelch,*Angew. Chem. Int. Edit.*, 2002, **41**, 2034-2057.
23. J. Leng, X. Lan, Y. Liu and S. Du,*Prog. Mater. Sci.*, 2011, **56**, 1077-1135.
24. J. Hu, Y. Zhu, H. Huang and J. Lu,*Prog. Polym. Sci.*, 2012, **37**, 1720-1763.
25. A. Lendlein and R. Langer,*Science*, 2002, **296**, 1673-1676.
26. A. Garle, S. Kong, U. Ojha and B. M. Budhlall,*ACS Appl. Mater. Inter.*, 2012, **4**, 645-657.
27. J. Li, J. A. Viveros, M. H. Wrue and M. Anthamatten,*Adv. Mater.*, 2007, **19**, 2851-2855.
28. M. C. Serrano, L. Carbajal and G. A. Ameer,*Adv. Mater.*, 2011, **23**, 2211-2215.
29. T. Xie,*Polymer.*, 2011, **52**, 4985-5000.
30. D. L. Thomsen, P. Keller, J. Naciri, R. Pink, H. Jeon, D. Shenoy and B. R. Ratna, *Macromolecules*, 2001, **34**, 5868-5875.
31. D. K. Shenoy, L. Thomsen III, A. Srinivasan, P. Keller and B. R. Ratna,*Sens. Actuat. A: Phys.*, 2002, **96**, 184-188.
32. M. Behl, K. Kratz, J. Zotzmann, U. Nochel and A. Lendlein,*Adv. Mater.*, 2013, **25**, 4466-4469.
33. H. Zhuo, J. Hu and S. Chen,*J. Mater. Sci.*, 2011, **46**, 3464-3469.
34. T. Chung, A. Romo-Uribe and P. T. Mather,*Macromolecules*, 2008, **41**, 184-192.
35. K. M. Lee, P. T. Knight, T. Chung and P. T. Mather,*Macromolecules*, 2008, **41**, 4730-4738.
36. J. Li, W. R. Rodgers and T. Xie,*Polymer*, 2011, **52**, 5320-5325.
37. S. Pandini, S. Passera, M. Messori, K. Paderni, M. Toselli, A. Gianoncelli, E. Bontempi and T. Riccò,*Polymer*, 2012, **53**, 1915-1924.

Journal of Materials Chemistry B Accepted Manuscript

38. M. Ebara, K. Uto, N. Idota, J. M. Hoffman and T. Aoyagi,*Adv. Mater.*, 2012, **24**, 273-278.
39. K. A. Davis, K. A. Burke, P. T. Mather and J. H. Henderson,*Biomaterials*, 2011, **32**, 2285-2293.
40. C. Min, W. Cui, J. Bei and S. Wang,*Polym. Adv. Technol.*, 2005, **16**, 608-615.
41. S. Neuss, I. Blomenkamp, R. Stainforth, D. Boltersdorf, M. Jansen, N. Butz, A. Perez-Bouza and R. Knüchel,*Biomaterials*, 2009, **30**, 1697-1705.
42. S. Zhou, X. Deng and H. Yang,*Biomaterials*, 2003, **24**, 3563-3570.
43. X. Yang, L. Wang, W. Wang, H. Chen, G. Yang and S. Zhou,*ACS Appl. Mater. & Inter.*, 2014.
44. X. Yu, S. Zhou, X. Zheng, T. Guo, Y. Xiao and B. Song,*Nanotechnology*, 2009, **20**, 235702.
45. T. Gong, W. Li, H. Chen, L. Wang, S. Shao and S. Zhou,*Acta Biomater.*, 2012, **8**, 1248-1259.
46. S. Shao, S. Zhou, L. Li, J. Li, C. Luo, J. Wang, X. Li and J. Weng,*Biomaterials*, 2011, **32**, 2821-2833.
47. A. Duda, Z. Florjanczyk, A. Hofman, S. Slomkowski and S. Penczek, *Macromolecules*, 1990, **23**, 1640-1646.
48. M.-H. Thibault and F.-G. Fontaine,*Dalton Trans.*, 2010, **39**, 5688-5697.
49. M. Labet and W. Thielemans,*Chem. Soc. Rev.*, 2009, **38**, 3484-3504.
50. T. Xie,*Nature*, 2010, **464**, 267-270.
51. T. Xie, K. A. Page and S. A. Eastman,*Adv. Funct. Mater.*, 2011, **21**, 2057-2066.
52. P. Miaudet, A. Derré, M. Maugey, C. Zakri, P. M. Piccione, R. Inoubli and P. Poulin,*Science*, 2007, **318**, 1294-1296.
53. S. Rezanejad and M. Kokabi,*Eur. Poly. J.*, 2007, **43**, 2856-2865.
54. R. M. Baker, J. H. Henderson and P. T. Mather,*J. Mater. Chem. B*, 2013, **1**, 4916-4920.
55. M. Nagata and Y. Yamamoto,*Macromol. Chem. Phys.*, 2010, **211**, 1826-1835.
56. M. Y. Razzaq, M. Behl, K. Kratz and A. Lendlein,*Adv. Mater.*, 2013, **25**, 5730-5733.
57. M. Behl, M. Y. Razzaq and A. Lendlein,*Adv. Mater.*, 2010, **22**, 3388-3410.

Journal of Materials Chemistry B Accepted Manuscript

This journal is © The Royal Society of Chemistry 2012